Generation of the primary hair follicle pattern

Chunyan Mou*, Ben Jackson*, Pascal Schneider†, Paul A. Overbeek‡, and Denis J. Headon*§

*Faculty of Life Sciences, University of Manchester, Manchester M13 9PT, United Kingdom; †Department of Biochemistry, BIL Biomedical Research Center, University of Lausanne, CH-1066 Epalinges, Switzerland; and ‡Department of Molecular and Cellular Biology, Baylor College of Medicine, Houston, TX 77030

Edited by Kathryn V. Anderson, Sloan–Kettering Institute, New York, NY, and approved May 8, 2006 (received for review January 31, 2006)

Hair follicles are spaced apart from one another at regular intervals through the skin. Although follicles are predominantly epidermal structures, classical tissue recombination experiments indicated that the underlying dermis defines their location during development. Although many molecules involved in hair follicle formation have been identified, the molecular interactions that determine the emergent property of pattern formation have remained elusive. We have used embryonic skin cultures to dissect signaling responses and patterning outcomes as the skin spatially organizes itself. We find that ectodysplasin receptor (Edar)–bone morphogenetic protein (BMP) signaling and transcriptional interactions are central to generation of the primary hair follicle pattern, with restriction of responsiveness, rather than localization of an inducing ligand, being the key driver in this process. The crux of this patterning mechanism is rapid Edar-positive feedback in the epidermis coupled with induction of dermal *BMP4*/*7*. The BMPs in turn repress epidermal *Edar* and hence follicle fate. Edar activation also induces connective tissue growth factor, an inhibitor of BMP signaling, allowing BMP action only at a distance from their site of synthesis. Consistent with this model, transgenic hyperactivation of Edar signaling leads to widespread overproduction of hair follicles. This Edar–BMP activation–inhibition mechanism appears to operate alongside a labile prepattern, suggesting that Edar-mediated stabilization of β-catenin active foci is a key event in determining definitive follicle locations.

pattern formation | reaction–diffusion | skin development

Periodic patterns are a recurring theme in anatomical organization. Examples in diverse organisms include insect bristles, mammalian hairs, the location of leaves on a plant, and the location of stomata on those leaves. In all of these cases the position of each element in the pattern is defined relative to the others rather than to an absolute anatomical location. With regular patterns found so widely in nature, a key question in developmental biology is how an ordered array of structures can be generated from an initially homogeneous field of cells. In general terms, such patterns can be generated by using two signals with different ranges of action (1, 2). These activation–inhibition systems rely on an activator that promotes (*i*) its own synthesis, (*ii*) assumption of a given cell fate, and (*iii*) synthesis of an inhibitor of this fate. Crucial in generating a spatial pattern is that the activator acts locally, whereas the inhibitor acts at a distance from its site of production. These types of molecular interactions are predicted to be capable of generating a periodic pattern by amplifying stochastic asymmetries in initial concentrations of activator and inhibitor (1).

Cells on the surface of mammalian embryos are competent to become either hair follicle or surface epidermis. They coordinate their fate choices to yield a stippled pattern of follicles, relying on communication within the skin rather than any external positional information. Recombination of epidermal and dermal components of embryonic skin established that communication between these cell layers is absolutely required for initiation of hair and feather development and that the dermis is responsible for inducing morphological changes in the epidermis (3, 4).

Many molecules that play a role in hair follicle development have been identified (5–8), but the regulatory relationships between signaling pathways involved in this process are largely unknown. This is a particularly important problem because it is the interactions between molecules, rather than the intrinsic function of any individual gene product, that is responsible for orchestrating pattern formation. One such signaling pathway, composed of the extracellular ligand ectodysplasin (Eda), its receptor Edar, and its cytoplasmic signaling adapter Edar-associated death domain (Edaradd), is required for development of a specific subset of hair follicles. Mutation of any of these three genes, all of which are specifically expressed in the epidermis, causes identical ectodermal dysplasia phenotypes in mouse and human (9–12). This phenotype includes a complete absence of primary hair follicles, which in mouse form between embryonic day (E) 13 and E16. It appears that *Edar* mutant epidermis retains its naïve state until E17, when secondary follicles begin to develop (10, 13). Secondary follicle formation has a distinct genetic basis, with mutations in *Noggin* (14) or *Lef1* (15) allowing primary hair follicle initiation but blocking that of secondary follicles.

Here we study the role of the Edar pathway in follicle patterning using embryonic skin cultures. The culture system allows experiments of short duration with a defined start point. This feature is particularly important for studying signal responses because it can distinguish the proximal effects of an experimental manipulation from those that are a secondary consequence caused by alteration of cell fates. We find that spatial organization in the epidermis is achieved by modulation of signal receptivity, with Edar–bone morphogenetic protein (BMP) activation–inhibition interactions driving the patterning process.

Results

Restriction of Eda Responsiveness Regulates Hair Follicle Density. Although activation–inhibition systems are generally predicted to rely on differential ligand availability, the ligand in this system, Eda, is a poor candidate for conveying positional information. *Eda* is widely expressed in the epidermis (13) and, when applied in a diffusible form, allows pattern formation in culture (16) and *in vivo* (17). Consequently, we considered dynamic *Edar* expression as a means to generate a punctate cell fate pattern. Before hair follicle initiation *Edar* is evenly expressed through the skin, but as a pattern emerges it becomes up-regulated in follicle primordia and down-regulated in surrounding cells. This dynamic expression itself depends on Edar signal transduction because it is not observed in $Edaradd^{-/-}$ embryos (Fig. 1*A*). Thus, as patterning takes place cells display one of three expression states; those with undetectable *Edar* are likely excluded from a hair follicle fate, those with high-level expression are committed to this fate, and those with moderate expression remain competent to assume either fate. Quantitative RT-PCR

Conflict of interest statement: No conflicts declared.

This paper was submitted directly (Track II) to the PNAS office.

Abbreviations: BMP, bone morphogenetic protein; CTGF, connective tissue growth factor; Eda, ectodysplasin; Edar, Eda receptor; Edaradd, Edar-associated death domain; qPCR, quantitative RT-PCR; E*n*, embryonic day *n*.

§To whom correspondence should be addressed. E-mail: denis.headon@manchester.ac.uk.

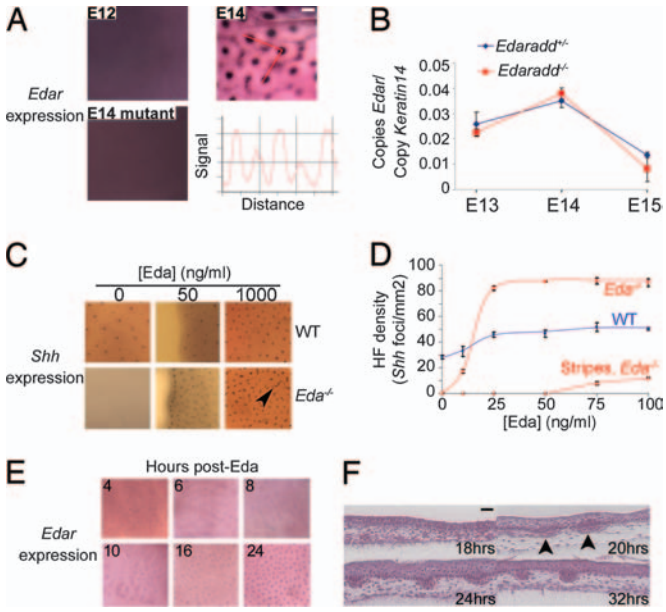

Fig. 1. Modulation of Eda responsiveness in developing skin. (*A*) *Edar* expression in E12 WT, E14 WT, and E14 *Edaradd*$^{-/-}$ mutant skin and semi-quantitative analysis of *Edar* signal intensity along the red line. (Scale bar: 100 μm.) (*B*) *Edar* expression levels in skin from *Edaradd*$^{-/-}$ and *Edaradd*$^{+/-}$ embryos, normalized to *Keratin14*. (*C*) *Shh* expression in WT and *Eda*$^{-/-}$ skin cultures treated with recombinant Eda protein. *Eda*$^{-/-}$ skin displays an edge effect, with *Shh*-expressing foci aligned along the margin of the explant (*Lower Center*). High concentrations of Eda cause formation of stripes in mutant skin (arrowhead). Each panel shows 1 mm^2. (*D*) Hair follicle densities induced by recombinant Eda in E14 WT and *Eda*$^{-/-}$ skin. Error bars show SEM. (*E* and *F*) Timing of patterning and morphogenetic events. (*E*) *Edar* expression in E14 *Eda*$^{-/-}$ skin cultures after administration of 50 ng/ml Eda. Each panel shows 1 mm^2. (*F*) Sectioned *Eda*$^{-/-}$ skin after Eda administration. The first morphological indication of hair follicle formation is condensation of cells to form placodes (arrowheads). (Scale bar: 25 μm.)

(qPCR) revealed that skin of *Edaradd*$^{-/-}$ embryos expresses the same amount of *Edar* as that of their heterozygous littermates (Fig. 1*B*). This result illustrates that while pattern formation dramatically reorganizes *Edar* expression, it balances focal up-regulation with widespread down-regulation such that the total level of transcript is conserved. These findings raise the possibility that follicle patterning is controlled by restriction of competence to respond to Eda, with nascent follicles blocking *Edar* expression, and therefore follicle fate, in their surroundings.

If restriction of *Edar* to follicles and its down-regulation in their surrounding cells are key events in pattern formation, then WT skin that already contains follicle primordia should be less competent than *Eda* mutant skin to produce follicles in response to exogenous Eda. We cultured WT and *Eda*$^{-/-}$ E14 dorsal skin in various concentrations of recombinant Eda and assessed hair follicle density by detecting *Shh* (sonic hedgehog), an early hair follicle marker (18). WT skin contains ≈30 follicles per square millimeter in the absence of exogenous Eda, rising to 50 follicles per square millimeter at high Eda concentrations. *Eda*$^{-/-}$ skin is much more responsive to Eda, generating a maximum of 90 follicles per square millimeter (Fig. 1 *C* and *D*). At high concentrations of Eda, mutant skin generated stripe-like patterns, which were never observed in WT (Fig. 1*C*). Stripe formation is predicted in activation–inhibition systems when activator concentrations become saturating (19).

We noticed that treated mutant, but not WT, explants had follicle primordia aligned along their edges (Fig. 1*C*). This observation could be explained if cells along the margin of the tissue have an advantage in forming a follicle by being relieved of inhibitory factors from cells on one side. This edge effect, and the fact that *Eda*$^{-/-}$ skin can generate nearly twice as many follicles as WT, argues that final follicle locations are not predetermined in *Eda* mutants. These results suggest that application of exogenous Eda in this culture system initiates pattern formation, rather than simply revealing a preexisting, cryptic pattern. Taken together, these results link widespread expression of *Edar* with widespread competence to form a hair follicle and indicate that existing follicles cause restriction of this developmental potential.

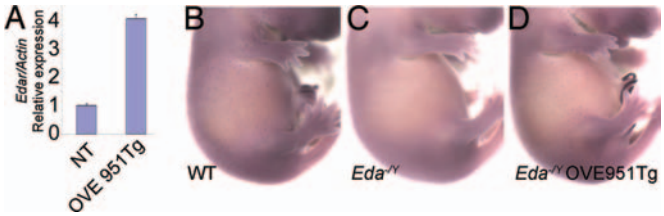

Fig. 2. Eda is dispensable for pattern formation. (*A*) qPCR determination of *Edar* expression in E14 *Edaradd*$^{-/-}$ nontransgenic (NT) and *Edaradd*$^{-/-}$ OVE951 skin. (*B*–*D*) *In situ* detection of *Shh* in WT (*B*), *Eda*$^{-/Y}$ (*C*), and *Eda*$^{-/Y}$ (*D*) OVE951 E15 embryos. Expression is detected only in the vibrissae of the mutant, but overexpression of *Edar* rescues the mutant phenotype, generating an accurate follicle pattern.

Timing of Patterning and Morphogenetic Events. To examine the rate of pattern formation and follicle morphogenesis we cultured *Eda*$^{-/-}$ skin with Eda and fixed samples at various time points. We found an ordered pattern of *Edar*-expressing foci appearing ≈10 h after Eda administration, after which the spots resolved and intensified to 24 h (Fig. 1*E*). The first definitive morphological indication of follicle formation, generation of a condensed placode, did not become visible until 20 h after Eda application (Fig. 1*F*). Thus, in this system a molecular prepattern precedes the appearance of morphologically identifiable placodes by ≈10 h.

Eda Is Dispensable for Pattern Formation. The transgenic line OVE951 carries a high copy number of a yeast artificial chromosome that includes the entire *Edar* locus (20) and consequently overexpresses *Edar* in its endogenous pattern (10). We quantified *Edar* expression in transgenic skin at E14, finding it to be 4-fold higher than in nontransgenic skin (Fig. 2*A*). We found that introducing this *Edar*-overexpressing locus into the *Eda*$^{-/-}$ line leads to rescue of primary follicle formation, as determined by *Shh* expression (Fig. 2 *B*–*D*). This finding shows that moderate *Edar* overexpression leads to ligand-independent signaling and illustrates that an accurate follicle pattern can be generated in the absence of Eda.

BMP Signaling Inhibits *Edar* Expression. The finding that *Edar* expression is undetectable in cells close to nascent follicles, whereas more distant cells express moderate levels of *Edar*, suggests that early hair follicles produce a diffusible inhibitor of *Edar* expression that restricts competence to assume this fate in surrounding cells. Two secreted ligands have been described as inhibitors of follicle formation: the BMPs (21, 22) and EGF (23). Both of these molecules block Eda-mediated follicle formation in culture (Fig. 3*A*), and so both are candidates for the *Edar*-repressing activity. We tested these molecules for inhibition of *Edar* expression in embryonic skin cultures. Importantly, the *Edar* inhibitor should act before commitment to follicle fate, and so it should repress the basal *Edar* expression observed before patterning. The up-regulated Edar expression observed in follicle primordia may be under a distinct regulatory control.

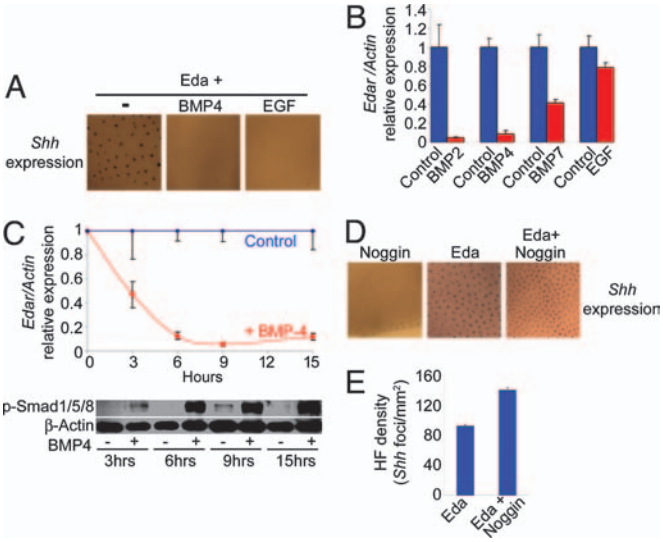

Fig. 3. BMPs inhibit *Edar* expression. (*A*) BMP4 and EGF inhibit follicle formation induced in $Eda^{-/-}$ skin by Eda. (*B*) Quantitation of *Edar* expression in E13 $Edaradd^{-/-}$ skin treated for 24 h with BMPs or EGF. (*C*) Time course inhibition of *Edar* by BMP4 and corresponding phospho-Smad levels. (*D*) *Shh* expression in $Eda^{-/-}$ skin treated with Noggin only, Eda only, or Eda plus Noggin for 24 h. (*E*) Hair follicle densities in $Eda^{-/-}$ skin treated with Eda with or without Noggin for 24 h. Error bars show SEM.

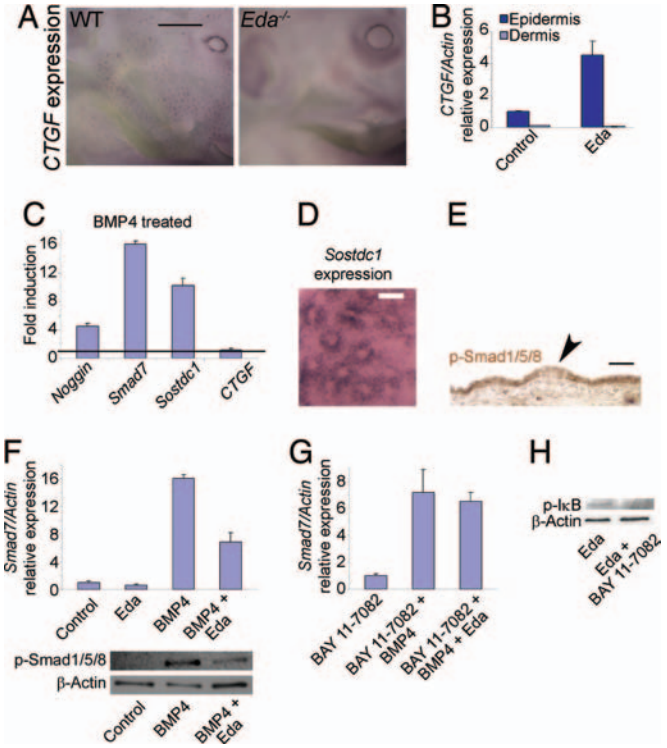

Fig. 4. BMPs act at a distance from the nascent follicle. (*A*) *CTGF* is expressed in hair follicle primordia in E15 WT, but not $Eda^{-/-}$, embryos. Expression is also seen in the eyelid. (Scale bar: 1 mm.) (*B*) Quantitation of *CTGF* mRNA in separated epidermis and dermis of mutant skin treated with 1,000 ng/ml Eda for 4 h. Edar stimulation induces *CTGF* expression in the epidermis, with little dermal expression observed. (*C*) Quantitation of gene expression in epidermis 5 h after addition of BMP4 to whole skin. *Noggin*, *Smad7*, and *Sostdc1* are induced by BMP treatment, whereas *CTGF* is not. (*D*) *Sostdc1* is expressed surrounding and away from follicle primordia 24 h after administration of Eda. (Scale bar: 100 μm.) (*E*) Immunodetection of phospho-Smad1/5/8 in the epidermis of E15 WT skin, with low levels in follicle placodes (arrowhead). (Scale bar: 100 μm.) (*F*) *Smad7* expression in epidermis 5 h after BMP4 with or without Eda application and corresponding epidermal Smad1/5/8 phosphorylation levels. Cotreatment with Eda suppresses BMP-induced *Smad7* activation and Smad1/5/8 phosphorylation. (*G*) *Smad7* expression in isolated epidermis 5 h after BMP4 with or without Eda application in the presence of the NF-κB inhibitor BAY 11-7082. (*H*) Bay 11-7082 blocks Eda-mediated IκBα phosphorylation in the epidermis. Error bars show SEM.

Because mutant skin exhibits only the widespread, moderate expression of *Edar* (Fig. 1*A*), we used it for these experiments. We found that the BMPs strongly repressed *Edar* expression, whereas EGF did not (Fig. 3*B*). BMP repression of *Edar* is rapid and correlates with levels of phospho-Smad1/5/8, the activated form of intracellular transducers of BMP signals (Fig. 3*C*).

To determine whether endogenous BMPs influence pattern formation we used Noggin, a specific inhibitor of BMPs 2, 4, and 7 (24). The maximum hair follicle density achieved by Eda treatment of $Eda^{-/-}$ skin was ≈90 per square millimeter (Fig. 1*D*). Cotreatment with Noggin breached this limit, allowing formation of 140 follicles per square millimeter (Fig. 3 *D* and *E*), without generation of stripes. This result demonstrates that endogenous BMPs restrict Eda responsiveness during pattern formation. Treatment with Noggin alone caused formation of small clusters of follicles in mutant skin, indicating that relief from BMP signaling is sufficient to allow some sporadic follicle formation in the absence of Edar activity (Fig. 3*D*).

BMPs Act at a Distance from the Follicle. Because the follicle itself produces BMPs (25) and has high *Edar* expression, it must employ a mechanism to evade BMP-driven *Edar* down-regulation. We found that connective tissue growth factor (CTGF), which binds to and inhibits BMPs in a manner analogous to that of Noggin (26), is expressed in hair follicle placodes (Fig. 4*A*) and is a rapidly up-regulated target of Edar signaling (Fig. 4*B*). In contrast to *CTGF*, other inhibitors of BMP signaling expressed in developing skin [*Noggin*, *Smad7*, and *Sostdc1* (sclerostin domain-containing 1)/*Ectodin*/*WISE* (25, 27)] are themselves transcriptional targets of BMP (Fig. 4*C*), likely acting as feedback inhibitors of the signaling pathway. Consistent with the idea that the placode is a BMP-privileged zone, the BMP target *Sostdc1* is expressed surrounding and away from, but not within, follicle sources of BMP (Fig. 4*D*), and phospho-Smad1/5/8 is detected in E15 interfollicular epidermis but is largely absent from nascent follicles (Fig. 4*E*). Cotreatment of skin cultures with Eda and BMP represses BMP induction of its target gene *Smad7*, with this weakening of BMP transcriptional responses accompanied by suppression of Smad phosphorylation (Fig. 4*F*). Eda's ability to inhibit BMP responses relies on activation of NF-κB, because pharmacological suppression of this transcription factor allows full BMP response in the presence of Eda (Fig. 4 *G* and *H*). This finding is consistent with a role for Eda target genes in BMP inhibition rather than any direct interference between components of the Eda and BMP signal transduction pathways. Thus, the BMPs act at a distance from their site of synthesis, and the early follicle itself is resistant to their action. Taken together, these experiments show that the BMPs display the characteristics of the inhibitory arm of an activation–inhibition loop.

Transcriptional Responses to Edar Signaling. If Edar functions in the activation arm of this loop, then it should be able to up-regulate its own expression, as well as that of the *BMP*s. To identify Edar signaling targets we treated $Eda^{-/-}$ cultures with Eda and analyzed gene expression in isolated epidermis and dermis. We used a high dose of Eda to achieve gross up-regulation of target gene expression rather than the relocation of expression observed during the physiological patterning process. *Edar* expres-

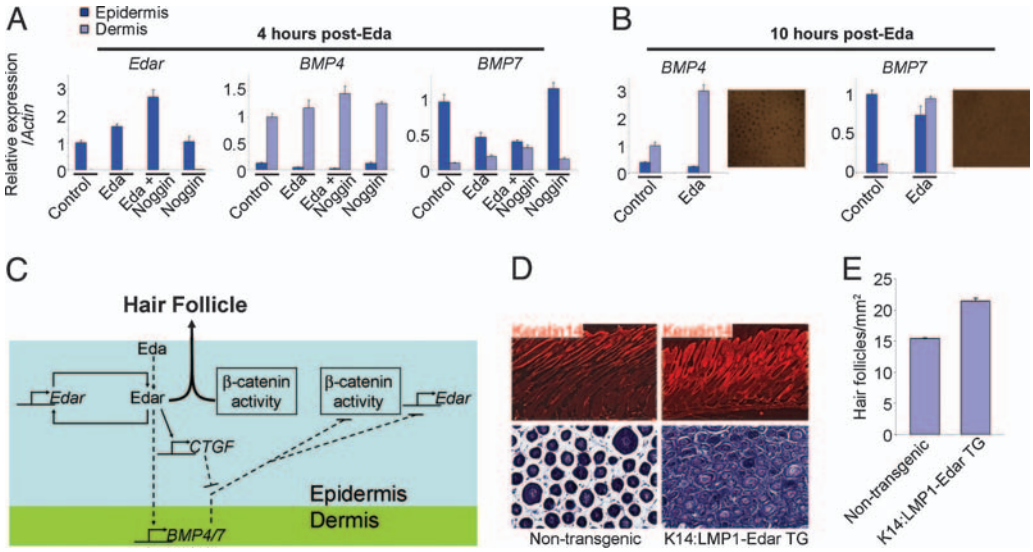

Fig. 5. Timing of transcriptional events, patterning model, and Edar hyperactivation. (*A*) *Eda*$^{-/-}$ mutant explants were cultured with or without Eda with or without Noggin for 4 h, and expression of *Edar*, *BMP4*, and *BMP7* was determined in separated epidermis and dermis. (*B*) *BMP* expression levels and location in mutant skin cultured with Eda for 10 h. The induced expression of *BMP4* and *BMP7* is punctate. (*C*) Proposed molecular interactions that generate the primary hair follicle pattern. Solid lines indicate cell-autonomous local interactions, and dotted lines indicate action at a distance. (*D*) Keratin14 immunostained longitudinal sections, and hematoxylin and eosin stained cross-sectioned dorsal skin of 10-day-old K14::LMP1-Edar transgenic and nontransgenic littermates. (*E*) Quantitation of hair follicle density in transgenic and nontransgenic mouse dorsal skin. Error bars show SEM.

sion was modestly activated by Eda within 4 h, with suppression of BMP signaling by cotreatment with Noggin enhancing this autoregulation (Fig. 5*A*). Analysis of *BMP* expression at 4 and 10 h found no significant changes in *BMP2* levels (data not shown), whereas *BMP4* was strongly activated in the dermis by 10 h (Fig. 5*B*). *BMP7* displayed the most rapid response to Eda, with initially low dermal levels up-regulated within 4 h (Fig. 5*A*) and strongly up-regulated at 10 h (Fig. 5*B*). The Eda-induced *BMP*s were focally expressed (Fig. 5*B*). Because *Edar* expression is restricted to the epidermis (Fig. 5*A*), dermal up-regulation of *BMP4* and *BMP7* must be an indirect effect. Interestingly, in addition to increasing overall BMP levels, up-regulation of *BMP7* in the dermal compartment would be predicted to enable formation of BMP4/7 heterodimers, which have been shown to be much more potent signals than BMP homodimers (28).

Based on these findings we propose a model for primary hair follicle patterning (Fig. 5*C*) in which the naïve embryonic epidermis evenly expresses molecules that activate (Eda and Edar) and inhibit (BMP) hair follicle identity. Edar undergoes local autoregulation and signal amplification, induces *CTGF*, and indirectly up-regulates *BMP* expression in the dermis. Local inhibition of BMP signaling forces their action at a distance to repress epidermal *Edar* and hence follicle fate. These interactions serve to amplify deviations in the initial conditions to generate a spatially organized follicle array.

We sought to incorporate β-catenin into this model because its activation is essential for follicle patterning and morphogenesis (29). We analyzed expression of *Axin2*, a direct β-catenin target gene (30), and found an ordered array of *Axin2*-positive foci in WT E15 epidermis. *Eda*$^{-/-}$ skin had occasional clusters of these *Axin2* foci, suggesting that some punctate β-catenin activity is present in the absence of Edar signaling. In culture these foci were suppressed by BMP and enhanced or stabilized by Eda. Thus, some prepatterned β-catenin activity appears independent of Edar function. This observation apparently contradicts our model in which Edar function regulates patterning decisions. One possibility is that these *Axin2* foci are proposed follicle locations that have the potential to be stabilized by Edar. To determine when a final follicle pattern becomes fixed we cut cultured skin at different times after Eda application and looked for alignment of follicles along the newly generated edge. Edge effects were observed when skin had been exposed to Eda for $<$10 h, whereas after this time the ability of the pattern to be reconfigured in response to perturbation of the field is lost (these data are in Fig. 6, which is published as supporting information on the PNAS web site). These findings indicate that a labile prepattern exists in the absence of Edar signaling but that it takes $>$10 h of molecular negotiation in the presence of Eda to fix a definitive pattern.

The proposed model considers restriction of Edar activity as a pivotal event in patterning. A prediction that it makes, therefore, is that widespread Edar activation should lead to widespread assumption of hair follicle fate. We generated transgenic mice expressing a cDNA composed of the intracellular domain of Edar fused to the transmembrane domains of LMP1, a viral protein that confers ligand-independent signaling when fused to cell-surface receptors (31). This cDNA was expressed in the basal layer of the epidermis by using the Keratin14 promoter. Three independent founder mice displayed thickened, scaly skin and because of ill health had to be killed within 20 days of birth. Sectioning revealed that the skin of these animals was consumed with hair follicle down-growths, the follicles packed against one another with essentially no intervening spaces (Fig. 5*D*). Quantitation of follicles in transgenic dorsal skin showed that it has a density ≈40% greater than that of nontransgenic littermates (Fig. 5*E*). This generation of supernumerary follicles confirms the importance of restricting Edar signaling in generation of an appropriately patterned hair follicle array.

Discussion

We propose a receptivity-driven model for hair follicle formation in which regulation of *Edar* expression is pivotal. Other activation–inhibition systems that have been studied at a molecular level, such as determination of the branched feather structure (32) or vertebrate left–right asymmetry (33), rely on differential diffusion properties of two secreted ligands. In contrast, modulation of a receiving cell's responsiveness to a widely available signal is central to our model.

Such patterning mechanisms rely on a differential range of activating and inhibitory molecules. Edar and β-catenin are restricted to the cell in which they are produced, whereas CTGF and the BMPs are secreted molecules. This property suggests that CTGF action must be spatially restricted. Restriction could be achieved by CTGF immobilization on extracellular matrix components or by diffusion of CTGF–BMP complexes with subsequent release of active BMPs. The observation that mutant and WT embryonic skin have the same levels of Edar expression (Fig. 1*B*) is best explained by the fact that, although Eda up-regulates *Edar* expression, it also induces *BMP*s, which feed back to inhibit *Edar*.

The culture method we used allows synchronization of follicle formation and makes the skin accessible to experimental manipulations. However, it is important that observations from such *ex vivo* systems are correlated with the findings made in intact animals. In particular, application of recombinant proteins mimics transgenic gain of function approaches, whereas loss-of-function experiments are essential to understanding endogenous functions. In whole animals ablation of Edar signaling specifically blocks primary hair follicle formation (10), whereas suppression of β-catenin activation prevents formation of all follicle types (29). Consistent with an inhibitory role for BMPs in the patterning process, deletion of BMP receptor genes in embryonic epidermis causes an increase in follicle density by the end of the primary wave of follicle formation at E16 (34). In addition, deletion of *Noggin*, presumably leading to enhanced BMP signaling, reduces hair follicle numbers. However, *Noggin* mutation specifically ablates secondary follicles while allowing primary follicles to form (14). This mutant phenotype may indicate that Noggin is the chief BMP inhibitor used by secondary follicles to avoid BMP autostimulation, while primary hair follicles instead employ CTGF. *CTGF*-null mice display skeletal abnormalities and die at birth (35), but their skin phenotype has not been described.

In our experiments, manipulation of signaling activities enabled modulation of placode densities over a wide range, from 30 per square millimeter to 140 per square millimeter. This plasticity, as well as the alignment of follicles along the boundary of dissected skin explants, indicates that their ultimate locations have not been defined in *Eda* mutant skin. However, we did find sporadic *Axin2* expression, indicative of patterned β-catenin activity, in the absence of Eda. These foci may be the same cells that were recently identified as initiating, but failing to maintain, very early follicle morphogenesis in *Edar* mutant skin (36). The malleability of follicle position in response to experimental perturbation suggests that this prepattern does not necessarily represent the final hair follicle array. *Axin2*-expressing foci might be "proposed" follicle locations that become fixed or otherwise as Edar function is restricted in the skin. Although the relationship between β-catenin and Edar remains to be fully elucidated, one link between these signaling modules is the finding that BMP inhibits formation of *Axin2* foci, whereas Edar suppresses BMP responses. Thus, Edar could enhance β-catenin function indirectly by shielding it from BMP action. The placodes induced by Noggin in Eda mutant skin (Fig. 3*D*) may represent such a stabilization of *Axin2* foci.

The up-regulation of *Edar* observed in early placodes is likely to influence its signaling properties, as illustrated by its overexpression under control of native regulatory elements in the OVE951 line. The ability of moderately elevated receptor levels to compensate for Eda deficiency suggests that receptor up-regulation confers ligand-independent signaling. Thus, the autoactivation of *Edar* expression that normally occurs in early placodes may be sufficient to allow Eda-independent signal transduction, helping establish commitment to a follicle fate. Our model predicts that ectopic follicles are not produced in this case, despite autonomous Edar signaling, because its expression remains susceptible to BMP inhibition. The K14:LMP1-Edar line was engineered to have ligand-independent signaling but produced a much more dramatic phenotype of ectopic follicle formation. This observation is in accordance with our model because the promoter driving expression is not susceptible to down-regulation by BMPs. The skin of this transgenic line is essentially unpatterned in the sense that follicles simply pack all available space rather than spatially regulating their locations. The Edar-induced phenotype contrasts with the effects of widespread transgenic activation of β-catenin, which causes growth of new follicles only in adult mouse skin, but does not lead to formation of ectopic follicles during the embryonic period (37). This finding suggests that restriction of β-catenin activation is not limiting in defining hair placode locations, although its activity is clearly necessary for follicle formation.

In this work, we provide a framework onto which to build other factors involved in hair follicle development as their relationships to the Edar and BMP pathways are uncovered. More broadly, it is likely that variations on this molecular network underlie pattern formation in scale and feather development and generation of tooth morphology. In addition, our findings of epidermal–dermal communication from the earliest stages of patterning indicate a decisive role for both tissues and contradict the simple view that positional information is first generated in the dermis and then conveyed to a passive epidermis.

Methods

Animals. WT, $Eda^{Ta/Ta}$, and $Edaradd^{cr/cr}$ lines were on the FVB/N background. OVE951 transgenic animals were used to detect *Edar* by *in situ* hybridization. *Eda* is on the X chromosome; for brevity $Eda^{-/-}$ is used in the text to refer to female $Eda^{-/-}$ and male $Eda^{-/Y}$ animals. For timed matings the day on which a vaginal plug was detected was counted as day 0. K14:LMP1-Edar transgenic mice were generated as described (38).

***In Situ* Hybridization.** Samples were fixed in 4% paraformaldehyde in PBS overnight at 4°C. Hybridization was performed as described (39). *In situ* hybridizations were photographed, and follicle density was determined by counting the number of *Shh*-expressing foci in a square of side 1 mm. Data from at least three independent skin explant cultures were used for each follicle density determination. Skin edges were not included in the analysis. Stripes were included in counts as a single follicle.

qPCR. RNA was reverse-transcribed by using random primers and AMV reverse transcriptase (Roche) in a 20-μl reaction. Reactions were diluted 10-fold, and 5 μl was used as template for each qPCR. TaqMan probes were supplied by Applied Biosystems. The probes used were as follows: *βActin* (4352341E), *BMP2* (Mm01962382_s1), *BMP4* (Mm00432087_m1), *BMP7* (Mm00432102_m1), *CTGF* (Mm00515790_g1), *Edar* (Mm00839685_m1), *Keratin14* (Mm00516876_m1), *Noggin* (Mm00476456_s1), *Smad7* (Mm00484741_m1), and *Sostdc1* (Mm00840254_m1). Twenty-microliter reactions were performed in triplicate by using an OpticonII thermocycler, with at least three biological replicates used to determine each data point. We did not observe changes in the total amount of *βActin* expression across the different experimental treatments. For each experiment control and treated samples came from the same litter. Relative or absolute amounts of normalizer and test transcripts were calculated from a standard curve.

Skin Organ Culture and Treatments. Dorsal skin was dissected, placed onto an MF-Millipore filter on a metal grid, and submerged in DMEM plus 5% FBS in a center-well dish (Falcon) at 37°C and 5% CO_2. Epidermal–dermal separations were performed by incubating skin samples at 37°C for 10 min with 2 mg/ml dispase (GIBCO). Tissues were homogenized in TRI reagent (Sigma) to isolate total RNA and proteins. Recombinant

EdaA1 (17) was used at 50 ng/ml for *in situ* hybridizations and histology and at 1,000 ng/ml for analysis of transcriptional targets by qPCR. Recombinant BMPs and EGF were used at 500 ng/ml, and Noggin was used at 1,000 ng/ml. Human BMP2, human BMP4, human BMP7, mouse EGF, and mouse Noggin proteins were from R & D Systems. For experiments involving cotreatment with Noggin the cultures were pretreated with Noggin for 2 h before the addition of Eda. BAY 11-7082 (Calbiochem) was used at 20 μM.

Histology and Immunohistochemistry. Samples were fixed in 4% paraformaldehyde in PBS at 4°C overnight and then dehydrated and embedded in paraffin wax. Six-micrometer sections were stained with hematoxylin and eosin, 1/1,000 FITC-conjugated anti-Keratin14 (Covance), or 1/100 rabbit anti-phospho-Smad1/5/8 (Cell Signaling Technology). Rabbit primary antibody was detected by using 1/200 biotinylated goat anti-rabbit (Upstate Biotechnology) and ABC peroxidase (Vector Laboratories).

Western Blotting. Protein samples were run on a 12% SDS/polyacrylamide gel and transferred to a nitrocellulose membrane. Blots were blocked in 5% skimmed milk in TBS/0.1% Tween 20 for 1 h and then probed with primary antibody [1/25,000 mouse monoclonal anti-β*Actin*-horseradish peroxidase AC-15 (Sigma), 1/1,000 anti-phospho-Smad1/5/8, and 1/2,000 mouse anti-phospho-IκBα 5A5 (Cell Signaling Technology)] in TBS/0.1% Tween 20 overnight. Signal was detected by using horseradish peroxidase-conjugated secondary antibodies and chemiluminescent substrate.

We thank C. M. Chuong, M. Dixon, D. Garrod, E. Harris, A. Hurlstone, H. Meinhardt, C. Thompson, and R. Widelitz. This work was supported by Wellcome Trust Grant 075220/Z.

1. Meinhardt, H. & Gierer, A. (2000) *BioEssays* **22,** 753–760.
2. Salazar-Ciudad, I. & Jernvall, J. (2002) *Proc. Natl. Acad. Sci. USA* **99,** 8116–8120.
3. Sengel, P. (1976) *Morphogenesis of Skin* (Cambridge Univ. Press, Cambridge, U.K.).
4. Sengel, P. (1990) *Int. J. Dev. Biol.* **34,** 33–50.
5. Fuchs, E., Merrill, B. J., Jamora, C. & DasGupta, R. (2001) *Dev. Cell* **1,** 13–25.
6. Millar, S. E. (2002) *J. Invest. Dermatol.* **118,** 216–225.
7. Millar, S. E. (2005) *PLoS Biol.* **3,** e372.
8. Schmidt-Ullrich, R. & Paus, R. (2005) *BioEssays* **27,** 247–261.
9. Headon, D. J., Emmal, S. A., Ferguson, B. M., Tucker, A. S., Justice, M. J., Sharpe, P. T., Zonana, J. & Overbeek, P. A. (2001) *Nature* **414,** 913–916.
10. Headon, D. J. & Overbeek, P. A. (1999) *Nat. Genet.* **22,** 370–374.
11. Monreal, A. W., Ferguson, B. M., Headon, D. J., Street, S. L., Overbeek, P. A. & Zonana, J. (1999) *Nat. Genet.* **22,** 366–369.
12. Kere, J., Srivastava, A. K., Montonen, O., Zonana, J., Thomas, N., Ferguson, B., Munoz, F., Morgan, D., Clarke, A., Baybayan, P., *et al.* (1996) *Nat. Genet.* **13,** 409–416.
13. Laurikkala, J., Pispa, J., Jung, H. S., Nieminen, P., Mikkola, M., Wang, X., Saarialho-Kere, U., Galceran, J., Grosschedl, R. & Thesleff, I. (2002) *Development (Cambridge, U.K.)* **129,** 2541–2553.
14. Botchkarev, V. A., Botchkareva, N. V., Sharov, A. A., Funa, K., Huber, O. & Gilchrest, B. A. (2002) *J. Invest. Dermatol.* **118,** 3–10.
15. van Genderen, C., Okamura, R. M., Farinas, I., Quo, R. G., Parslow, T. G., Bruhn, L. & Grosschedl, R. (1994) *Genes Dev.* **8,** 2691–2703.
16. Mustonen, T., Ilmonen, M., Pummila, M., Kangas, A. T., Laurikkala, J., Jaatinen, R., Pispa, J., Gaide, O., Schneider, P., Thesleff, I., *et al.* (2004) *Development (Cambridge, U.K.)* **131,** 4907–4919.
17. Gaide, O. & Schneider, P. (2003) *Nat. Med.* **9,** 614–618.
18. St Jacques, B., Dassule, H. R., Karavanova, I., Botchkarev, V. A., Li, J., Danielian, P. S., McMahon, J. A., Lewis, P. M., Paus, R. & McMahon, A. P. (1998) *Curr. Biol.* **8,** 1058–1068.
19. Meinhardt, H. (1989) *Development (Cambridge, U.K.)* **107,** Suppl., 169–180.
20. Majumder, K., Shawlot, W., Schuster, G., Harrison, W., Elder, F. F. & Overbeek, P. A. (1998) *Mamm. Genome* **9,** 863–868.
21. Jung, H. S., Francis-West, P. H., Widelitz, R. B., Jiang, T. X., Ting-Berreth, S., Tickle, C., Wolpert, L. & Chuong, C. M. (1998) *Dev. Biol.* **196,** 11–23.
22. Noramly, S. & Morgan, B. A. (1998) *Development (Cambridge, U.K.)* **125,** 3775–3787.
23. Kashiwagi, M., Kuroki, T. & Huh, N. (1997) *Dev. Biol.* **189,** 22–32.
24. Zimmerman, L. B., Jesus-Escobar, J. M. & Harland, R. M. (1996) *Cell* **86,** 599–606.
25. Botchkarev, V. A. & Sharov, A. A. (2004) *Differentiation* **72,** 512–526.
26. Abreu, J. G., Ketpura, N. I., Reversade, B. & De Robertis, E. M. (2002) *Nat. Cell Biol.* **4,** 599–604.
27. Laurikkala, J., Kassai, Y., Pakkasjarvi, L., Thesleff, I. & Itoh, N. (2003) *Dev. Biol.* **264,** 91–105.
28. Aono, A., Hazama, M., Notoya, K., Taketomi, S., Yamasaki, H., Tsukuda, R., Sasaki, S. & Fujisawa, Y. (1995) *Biochem. Biophys. Res. Commun.* **210,** 670–677.
29. Andl, T., Reddy, S. T., Gaddapara, T. & Millar, S. E. (2002) *Dev. Cell* **2,** 643–653.
30. Jho, E. H., Zhang, T., Domon, C., Joo, C. K., Freund, J. N. & Costantini, F. (2002) *Mol. Cell. Biol.* **22,** 1172–1183.
31. Gires, O., Zimber-Strobl, U., Gonnella, R., Ueffing, M., Marschall, G., Zeidler, R., Pich, D. & Hammerschmidt, W. (1997) *EMBO J.* **16,** 6131–6140.
32. Harris, M. P., Williamson, S., Fallon, J. F., Meinhardt, H. & Prum, R. O. (2005) *Proc. Natl. Acad. Sci. USA* **102,** 11734–11739.
33. Solnica-Krezel, L. (2003) *Curr. Biol.* **13,** R7–R9.
34. Andl, T., Ahn, K., Kairo, A., Chu, E. Y., Wine-Lee, L., Reddy, S. T., Croft, N. J., Cebra-Thomas, J. A., Metzger, D., Chambon, P., *et al.* (2004) *Development (Cambridge, U.K.)* **131,** 2257–2268.
35. Ivkovic, S., Yoon, B. S., Popoff, S. N., Safadi, F. F., Libuda, D. E., Stephenson, R. C., Daluiski, A. & Lyons, K. M. (2003) *Development (Cambridge, U.K.)* **130,** 2779–2791.
36. Schmidt-Ullrich, R., Tobin, D. J., Lenhard, D., Schneider, P., Paus, R. & Scheidereit, C. (2006) *Development (Cambridge, U.K.)* **133,** 1045–1057.
37. Gat, U., DasGupta, R., Degenstein, L. & Fuchs, E. (1998) *Cell* **95,** 605–614.
38. Tucker, A. S., Headon, D. J., Courtney, J. M., Overbeek, P. & Sharpe, P. T. (2004) *Dev. Biol.* **268,** 185–194.
39. Byrne, C., Tainsky, M. & Fuchs, E. (1994) *Development (Cambridge, U.K.)* **120,** 2369–2383.

Mou *et al.* 10.1073/pnas.0600825103.

Supporting Figure

File in this Data Supplement:

Supporting Figure 6

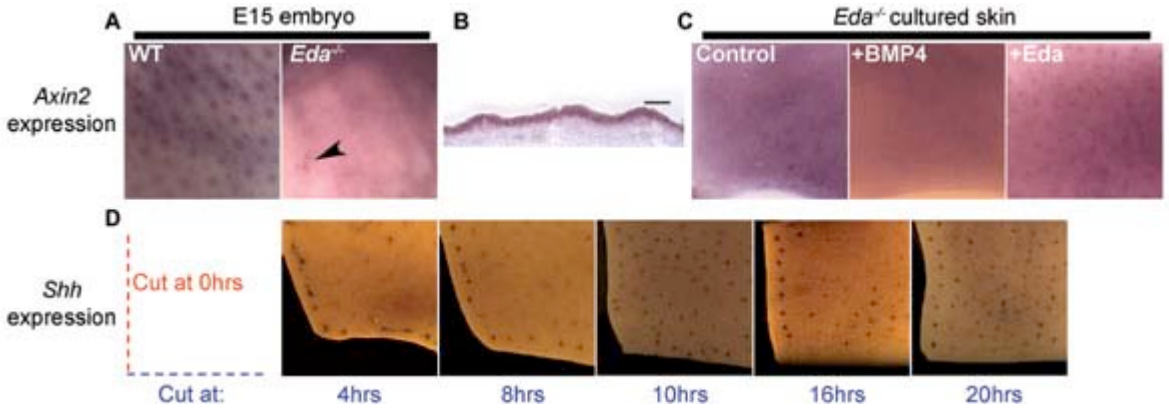

Fig. 6. A labile prepattern exists in the absence of Edar signaling. (*A*) *Axin2*, a direct b-catenin target, is detected in skin and follicles of E15 WT embryos and in occasional clustered foci (arrowhead) in *Eda*$^{-/-}$ mutants. (*B*) Sectioning revealed that *Axin2* expression is predominantly epidermal in WT E15 skin. (Scale bar: 100 mm.) (*C*) Cultured mutant skin also displays *Axin2* foci in the absence of Eda, and they are abolished by BMP4 administration. Application of 50 ng/ml Eda produces focal *Axin2* expression across the explant. (*D*) Time course edge effect experiment. Shown is *Shh* expression in *Eda*$^{-/-}$ explants cultured with 50 ng/ml Eda. The vertical edge was cut at time 0 as a positive control, and the horizontal edge was cut at various time points after Eda application. Samples were cultured for 24 h after the horizontal cut was made. The filter was digitally removed from the images by using PHOTOSHOP (Adobe Systems, San Jose, CA) to highlight the edges of the skin explants.